Antiviral Effects of Gelatin Stabilized Ferrous Sulfide Nanoparticles

Ting Tong
Huazhong Agricultural University
Shuangfei Deng
Huazhong Agricultural University
Xiaotong Zhang
Huazhong Agricultural University
Liurong Fang
Huazhong Agricultural University
Jiangong Liang (liangjg@mail.hzau.edu.cn)
Huazhong Agriculture University https://orcid.org/0000-0002-8210-0210
Shaobo Xiao
Huazhong Agricultural University

Research

Keywords: Ferrous sulfide nanoparticles, Antiviral mechanism, Porcine reproductive and respiratory syndrome virus, Inactivation, Adsorption, Invasion, Replication, Release

Posted Date: October 26th, 2021

DOI: https://doi.org/10.21203/rs.3.rs-970779/v1

Abstract

Ferrous sulfide nanoparticles (FeS NPs) are widely applied to environmental remediation, catalysis, energy storage and medicine because of their high reactivity, large specific surface area and low cost, arousing great interest of researchers. However, there is no literature reported on its application in the antiviral field. In the study, gelatin stabilized FeS nanoparticles (Gel-FeS NPs) were synthesized by co-precipitation of Fe^{2+} and S^{2-} in the aqueous phase with continuous stirring under anaerobic conditions. The as-prepared Gel-FeS NPs were good stabilization and dispersibility with the size distribution of 77.7 ± 16.4 nm, as determined by UV-Vis spectrometer, TEM, FTIR, XRD and XPS. We reported for the first time the virucidic and antiviral activity of Gel-FeS NPs. The Gel-FeS NPs with good dispersibility and biocompatibility were synthesized, and they exhibited effective inhibition on the proliferation of PRRSV by blocking the PRRSV outside the host cells. Moreover, the Fe^{2+} from degraded ferrous sulfide still displayed an antiviral effect, demonstrating the advantage as an antiviral nanomaterial of Gel-FeS NPs compared to other nanomaterials. This work highlighted the antiviral effect of Gel-FeS NPs, broaden the applications of iron-based nanoparticles for combating the virus.

Introduction

Respiratory virus infections and widespread epidemics have always posed an enormous threat to the public health system due to their strong infectious property. Porcine reproductive and respiratory syndrome virus (PRRSV) is an enveloped, single positive-stranded RNA virus, which belongs to the family *Arteriviridae* [1]. It has caused huge economic losses for the swine industry over three decades, the variability of RNA virus genome leads to persistent mutation and epidemic of PRRSV so that the prevention and treatment of the virus are still unsatisfactory [2]. It is critical to develop novel antiviral strategies against PRRSV by inactivating the virus from the initial stage of infection.

In recent years, a series of innovative nanomaterials have been reported with some potential activities against various viruses and played an important role in preventing and curing different viral infections [3–7]. DNA origami [8], graphene nanosheets [9, 10], fullerene nanospheres [11–13], macromolecular polymers [14], nano hydrogels [15–17], and other emerging materials [18, 19]. These nanomaterials can play an antiviral role in different processes of virus life cycle; however, the low synthesis yield and complex synthesis procedures of these materials restrict their further application. Therefore, the rapid and large-scale synthesis of antiviral nanomaterials with good reproducibility by one pot method obviously exhibited the rare advantage. In addition to the aforementioned antiviral materials, iron-based antiviral materials have attracted much attention. Iron ions are necessary trace elements that play a role in cell growth and in the prevention of cancer, cardiovascular disease and diabetes [20, 21].

It has been reported that the iron-based complexes have a specific antiviral effect in various viruses [22, 23], iron ions supplement therapy proved to be a promising antiviral method [24, 25]. However, the strong oxidicability of iron ions was harmful to cells to some extent, and iron supplement with ferrous ions has been extensively applied for the prevention and treatment of iron deficiency anemia [26, 27]. FeS has

been studied in many fields because of its specific physical and chemical properties, such as anti-tumor, energy, sewage treatment and so on[28, 29], but its antiviral effects have not been investigated. Considering that it can release ferrous ions, we assumed that FeS could be used as an antiviral agent. Meanwhile, gelatin has various attractive features as biomedical materials, for instance, biocompatibility, low immunogenicity, biodegradability, and ease of manipulation [30].

In this study, we reported an antiviral agent based on gelatin stabilized FeS NPs (Gel-FeS NPs), which was synthesized by co-precipitation methods. As expected, the Gel-FeS NPs exhibition good inhibition in PRRSV proliferation, it not only inactivates the virus particles but also affects the adsorption, invasion, and replication stages of PRRSV infection. To the best of our knowledge, we reported the virucidal and antiviral activity of ferrous-based nanoparticles for the first time. This work highlighted the antiviral effect of Gel-FeS NPs, demonstrating the application prospect of ferrous-based nanoparticles for combating the virus.

Materials And Methods

Chemicals and Reagents

Both $FeSO_4·7H_2O$ and $Na_2S_4·9H_2O$ were purchased from Sinopharm Chemical Reagent Co., Ltd., China. Gelatin was purchased from Shanghai Aladdin Chemistry Co. Ltd., China. The MARC-145 cell lines and PRRSV WUH3 strains were supplied by State Key Laboratory of Agricultural Microbiology (Wuhan, China). The cell lines were cultured in Dulbecco's modified Eagle's medium (DMEM) supplemented with 10% fetal bovine serum (FBS) and 1% penicillin/streptomycin, respectively. Further, incubation at 37 °C was performed using a humidified CO_2 incubator. All other the experimental chemicals not mentioned used were purchased from Sigma-Aldrich and had a high purity level, and all materials are used directly after purchase without further purification.

Preparation of Gel-FeS NPs

The preparation of stable Gel-FeS NPs was synthesized based on the reaction of $FeSO_4$ with Na_2S in the presence of gelatin through a co-precipitation method. Briefly, under continuous magnetic stirring and high purity nitrogen flow condition, 20.0 mL $FeSO_4$ (0.020 mol/L) solution and 50.0 mL gelatin (1.0 g/L) solution were added into three-necked flasks, the mixture was then stirred for 30 min to yield Fe^{2+}-gelatin complexes. Then, 20.0 mL Na_2S (0.020 mol/L) solution was added dropwise into the solution at an Fe-to-S molar ration of 1:1 to produce FeS nanoparticles [31]. Then the obtained liquid was centrifuged at 10000 r/min, and an appropriate amount of water was added to ultrasonically disperse the precipitate, which was centrifuged and washed three times and store the product at 4°C.

Characterization of Gel-FeS NPs

UV-Vis absorption spectra were recorded on a Shimadzu UV-2450 spectrometer (Japan). Spectrum data were detected from the wavelength of 600 nm to 200 nm by a 10 mm quartz cell. FTIR spectra were

recorded with a Thermo Fisher Nicolet Avatar-330 infrared spectrometer (USA) and scanned between 4000 to 500 cm^{-1}. TEM images were obtained by a JEOL JEM-2100F transmission electron microscope (Japan). The XRD pattern of the synthesized Gel-FeS NPs was constructed using a Shimadzu XRD-7000 X-ray diffractometer (Japan) with Cu Kα radiation at a voltage of 40 kV and a scanning rate of 10° min^{-1}. XPS scans spectra were carried out at a Thermo Fisher ESCALAB Xi X-ray photoelectron spectrometer (USA) to obtain the surface elemental composition and chemical state of the sample.

Cytotoxicity Assay

MARC-145 cells were seeded in 96-well plates to a confluence of approximately 80-90%, and the cells were incubated with different concentrations (0, 14.0, 28.0, 54.0, 108.0, 215.0, 430.0 μg/mL) of Gel-FeS NPs. Meanwhile, cells treated with the DMEM (2% FBS) were used as control. After incubating separately for 12, 24, 36 and 48 h, then standard MTT assay was used to evaluate cell viability [32].

Antiviral Assay

MARC-145 cells were incubated with different concentrations (0, 85.0, 170.0, 255.0, 340.0 μg/mL) of Gel-FeS NPs for 2 h at 37 °C. And PRRSV was pretreated with Gel-FeS NPs at 4 °C for 1 h in the meantime. Then, the cells were incubated with the pretreated PRRSV at the multiplicity of infection (MOI) of 1.0. After infection for 1 h, the inoculums were discarded, followed by two washes with DMEM, and the cells were incubated with Gel-FeS NPs at the corresponding concentration at 37 °C for 12, 24, 36 and 48 h, respectively. The cell samples were then collected or processed in different ways. For western blot assay, the cell samples were collected to detect the content of N or Nsp2 protein in the sample. For the indirect immunofluorescence assay, the cells were treated by antibody incubation and washing, then the samples were photographed with a fluorescence microscope. For plaque assay, the cells were freeze-thaw three times, then the samples were collected for measuring the virus content of the samples [33].

Indirect Immunofluorescence Assay

MARC-145 cells cultured in 24-well plates were collected at indicated time points, after three washes with PBS, the cells were treated by 4% paraformaldehyde for 15 min, and cells were permeabilized with precooled methanol at - 20 ℃ for 15 min. Next, the cells were blocked by 5% (w/v) BSA for 45 min and then detected with a mouse monoclonal antibody (primary antibodies) against the PRRSV N protein and Alexa Fluor 594-conjugated Donkey anti mouse lgG (secondary antibodies). Cell nucleus was stained by DAPI. The fluorescence images were acquired with Olympus FV10 laser scanning confocal microscope [34].

Plaque Assay

Briefly, MRAC-145 cells were seeded into 6-well plates and cultured until ~100 confluence, then the indicated samples were added to the plates by 10-fold gradient dilution with DMEM with 2% FBS. After 1.5 h incubation, the supernatant was discarded and the cells were washed three times with DMEM to

remove non-absorbed virus particles. Then 2 mL overlay medium (2 × DMEM: low melting point agarose 1.8% (w/w): FBS: penicillin-streptomycin = 48: 48: 3: 1) was added to each well, followed by cooling for 15 min at 4 °C to coagulated overlay medium. After incubation at 37 °C for 2~3 days, the cells were stained with 1.0 mL neutral red solution (0.50 mg/mL) for 1 h at 37 °C. Next, the supernatant was removed and the plates were stored at 4 °C overnight. Finally, numbers of plaques were counted and virus titers were calculated. All the virus titers were represented as plaque forming units (PFU/mL) [35].

Results

Characterization of Gel-FeS NPs

The gelatin stabilized FeS NPs were simply synthesized by co-precipitation method [36].The precursor containing ferrous ion of $FeSO_4$ and Na_2S are co-precipitate in nitrogen protected aqueous solutions under continuous stirring. Considering that FeS is unstable and easily oxidized in aqueous solution, we introduced biocompatible molecules gelatin into the reaction solution [31]. The introduced gelatin not only improves the dispersion and stability of FeS NPs, but also improves the biocompatibility. Fig. 1A presents UV-Vis spectra of $FeSO_4$, Na_2S, gelatin and Gel-FeS NPs, there are negligible absorption of the individual solutions of $FeSO_4$, Na_2S and gelatin at longer wavelength region over 250 nm. After mixing these three reagents and reaction, the black and turbid product was observed, and it had a strong absorbance in the wavelength range of 200-600 nm. Satisfactorily, although the Gel-FeS NPs storage at 4 °C for a week, there was no notable change in the UV-Vis spectra of Gel-FeS NPs, implying the good physically and chemically stabilization of Gel-FeS NPs in aqueous solution. The morphology and size distribution of Gel-FeS NPs were measured with TEM and dynamic light scattering (DLS) analyzer. The TEM image shows that Gel-FeS NPs were well-dispersed with nonuniform size in aqueous solution (Fig. 1B), which was consistent with the size distribution of the Gel-FeS NPs in the range of 77.7 ± 16.4 nm (inset map).

In order to further analyze the molecular structure and chemical bond information of Gel-FeS NPs, FTIR spectra of Gel-FeS NPs and gelatin were compared in the Fig. 1C to study the functional groups differences. The peaks appeared at 3434 cm^{-1} assigned to the O–H stretching vibrations from adsorbed water and the stabilizer gelation. The abundant O–H bonds in gelatin were contributed to the formation of strong intermolecular hydrogen bonds between gelatin and FeS NPs, which improved the stability of Gel-FeS NPs effectively. Moreover, the absorption peaks around at 1645 cm^{-1} and 1107 cm^{-1} attributed to the $-COO^-$ and C–O–C stretching vibrations, respectively. The FTIR results indicated that the gelation with functional groups such as O–H and $-COO^-$ were tightly attached to the surface of FeS NPs. The modification of gelatin provided electrostatic repulsion and steric hindrance for FeS to avoid oxidation and aggregation [37]. Subsequently, the XRD diffractogram of Gel-FeS NPs were analyzed (Fig. 1D), the two typical peaks at 2θ = 23.0° and 47.0° were indicative of FeS, and the diffraction peak at 2θ = 49.8° corresponding to (2 0 0) reflection of FeS, indicating the crystal form of FeS in the presence of gelatin

[38]. In addition, the peak appeared at $2\theta = 36.4°$ corresponded to iron oxides, probably attributing to partial oxidation of Gel-FeS NPs. These results show that Gel-FeS NPs is synthesis successful.

Subsequently, the components and surface functional groups of the Gel-FeS NPs were characterized by XPS analysis. The XPS full scans spectrum of Gel-FeS NPs is shown in the Fig. 2A, demonstrating five obvious peaks at binding energy of 163.30, 399.14, 530.98, 582.20 and 710.57 eV, which were corresponded to S 2p, C 1s, N 1s, O 1s and Fe 2p orbital, respectively. The high resolution XPS spectra of C 1s could be resolved into three peaks at 284.81, 286.12, 287.87, 288.52 eV, indicating the presence of C−C, C−O−C, C=O and O−C=O bonds in Gel-FeS NPs, respectively (Fig. 2B). Besides, Fig. 2C shows the high resolution XPS spectra of Fe 2p, the peak centered at 710.92 eV assigned to Fe(Ⅱ)−S species, which were the main forms of elements Fe in Gel-FeS NPs. And the peaks at 719.04 and 724.33 eV were attributed to Fe(Ⅲ)−O and Fe(Ⅱ)−O, respectively, implying the Gel-FeS NPs partly oxidized during the preparation and storage process as article reported [39]. Moreover, the peak at 161.50 eV was ascribed to FeS in high resolution XPS spectra of S 2p (Fig. 2D), corresponding to the analysis result of Fe 2p. Additionally, there were two peaks at 167.41 and 168.30 eV of SO_4^{2-}, which indicated that some sulphate impurities could not be removed thoroughly.

Inhibitory Effect of Ferrous Ion on PRRSV Proliferation

First, we verified the antiviral activity of ferrous ion, and investigated whether the synthetic raw materials $FeSO_4$, Na_2S and gelatin themselves can inhibit the proliferation of PRRSV. MARC-145 cells were selected, cell viability was monitored by the MTT assay to estimate the cytotoxicity of such raw material and to define experimental conditions. Since the raw material ferrous sulfate is easily oxidized, we choose ferrous ammonium sulfate solution to explore the biocompatibility of ferrous ions. In this way, we cultured MARC-145 cells in the presence of raw materials at different concentrations. Cells cultured in the absence of raw material were used as the control experiment. as the data result in **Fig. S1A**, the cell survival rate was about 75% at the concentration of 60.0 μg/mL, in addition, the cell viability is greatly reduced after incubation with 80.0 μg/mL of ferrous ions. However, there is little cytotoxicity at the concentration of 40.0 μg/mL, the concentration at 40.0 μg/mL was selected to explore the antiviral activity of three synthetic raw materials by indirect immunofluorescence assay.

As depicted in **Fig. S1B**, the red fluorescence signal representing PRRSV N protein reduced significantly after treatment with $FeSO_4$, whereas no visible differences were seen after treatment with Na_2S and gelatin, indicating that the $FeSO_4$ in synthetic raw materials of Gel-FeS NPs had antiviral activity on PRRSV. This result confirmed our hypothesis that ferrous ion has antiviral activity. And implied it is the Fe (II) in Gel-FeS NPs that plays a dominate role in inhibiting PRRSV proliferation.

Gel-FeS NPs Indicating Enhanced Biocompatibility

Cell viability was monitored by the MTT assay to estimate the cytotoxicity of the prepared particles and to define experimental conditions. After incubation with Gel-FeS NPs for 12, 24, 36, 48 h, the potential

cytotoxicity of Gel-FeS NPs on MARC-145 cells was detected by MTT assay. As depicted in Fig. 3, negligible cytotoxicity of the Gel-FeS NPs treated MARC-145 cells can be observed at the concentration below 430.0 μg/mL for 12, 24, 36 and 48 h. Compared with the cytotoxicity of the raw materials for Gel-FeS NPs synthesis, the biocompatibility of Gel-FeS NPs was significantly improved. According to the results of inductively coupled plasma-mass spectrometry (the experimental results are not shown in figures), the mass fraction of Fe in Gel-FeS NPs is 23.5%. We converted the content of Fe in Gel-FeS NPs, 430.0 μg/mL of Gel-FeS NPs contains 101.0 μg/mL iron element. In contrast, the modification of gelatin greatly improves the biocompatibility of ferrous ions.

Gel-FeS NPs Exhibit Inhibitory Effect on PRRSV Proliferation

Based on the results of the above cytotoxicity experiments and the concentration control of the prepared samples, we finally chose four concentrations (0, 85.0, 170.0, 255.0, 340.0 μg/mL) to study the antiviral activity of Gel-FeS NPs against PRRSV further. The inhibitory effect of Gel-FeS NPs on PRRSV was evaluated based on indirect immunofluorescence assay. In Fig. 4, it could be found that the red fluorescence signal representing PRRSV N protein in cytoplasm of MARC-145 cells declined significantly, showing the PRRSV content in cells reduced. There was almost no difference in the nuclei stained blue, which once again showed the good biocompatibility of Gel-FeS NPs.

Furthermore, the viral infectivity of PRRSV treated with Gel-FeS NPs was determined for quantitative analysis by plaque assay. Plaque reduction assay was carried out to evaluate the viral content in cells treated with Gel-FeS NPs or not as shown in Fig. 5, the titers of PRRSV decreased significantly in a dose-dependent manner by Gel-FeS NPs compared to the control groups, with the most predominant reduction of ~10^3-fold, that is an encouraging data. In a word, the above experimental results demonstrated the excellent antiviral effect of Gel-FeS NPs on PRRSV proliferation.

Gel-FeS NPs Inhibit PRRSV Proliferation by Multi-Stage

In order to explore the effect of Gel-FeS NPs on virus life cycle, the ability of direct inactivation PRRSV by Gel-FeS NPs was investigated. As described in the experimental method section of the supporting information, the results of plaque assay showed that PRRSV content decreased dramatically (Fig. 6A), indicating that Gel-FeS NPs possess virucidal activity in vitro.

The virus infection involves a series of stages, each of which may be a potential target of antiviral drugs. According to the reported life cycle characteristics of PRRSV and classical experimental methods, the effect of Gel-FeS NPs on each process of PRRSV proliferation was explored. The number of plaques can directly reflect the effect of Gel-FeS NPs on the proliferation of the virus. As shown in Fig. 6B and 6C, PRRSV content was decreased ~ 10-fold by Gel-FeS NPs during the two stages respectively, indicating that Gel-FeS NPs inhibit the adsorption and invasion processes of PRRSV.

Following invasion by receptor-mediated endocytosis and disassembly, replicase polyproteins were produced under the guide of PRRSV genome positive strand RNA. This process is isolated as a genome

replication process for PRRSV, so the level of PRRSV negative-sense RNA open reading frame 7 (ORF7) gene was quantified by RT-qPCR assay to assess the influence of Gel-FeS NPs on PRRSV replication. As described in Fig. 6D, the level of PRRSV negative-sense RNA ORF7 gene slightly decreased after treatment with Gel-FeS NPs at 340.0 mg/mL, suggesting that Gel-FeS NPs had a moderate inhibition effect on PRRSV replication. Finally, the release experiment of PRRSV progeny virus was carried out, the Gel-FeS NPs had no influence on PRRSV release because there was no significant change observed in the virus content in either intracellular or supernatant (Fig. 6E, F). In general, Gel-FeS NPs inhibited on PRRSV proliferation in MARC-145 cells by inhibiting the adsorption, invasion, replication but not the release stages of PRRSV.

Discussion

Iron is an essential element to maintain the basic cellular physiological activities in many organisms, such as oxygen transport, DNA replication, metabolic processes and so on [39]. Many proteins that have crucial roles in cellular physiology require iron to function [40]. And iron deficiency is associated with a series of diseases when iron-requiring enzymes become ineffective. For example, many HIV-positive patients suffer from iron deficiency which reduces their ability to resist viral infections, especially when the virus attacks immune cells [41]. Previous studies have shown that iron ions have antiviral activity, and iron is essential for activating the host's antiviral immune mechanism [42]. As an example, Fe(III) can effectively inhibit the replication of HSV-1 and bovine viral diarrhea virus (BVDV) [23]. It is speculated that Fe(III) may interact with viral RNA [43]. This interaction may hinder the replication of the viral genome. Extracellular iron such as FAC can also inhibit the infection of iron HIV-1 by inhibiting the release of HIV-1 from lysosomes and inhibit the replication of dengue virus by activating the activity of ROS in the intestinal epithelium of mosquitoes [24]. However, high concentration of iron ion may produce strong cytotoxicity. The survival rate of cells was less than 50% when they were cultured with 40 μg/mL ferrous ions. Therefore, how to improve the biocompatibility and antiviral effect of iron ion is of great significance for the application of iron ion in antiviral.

The research in this paper found that when ferrous ions are prepared into gelatin-modified ferrous sulfide nanoparticles, their biocompatibility and antiviral effects are significantly improved. The ferrous sulfide nanoparticles synthesized in this paper are between 60-90 nm, and their size is like that of virus particles, which can inhibit virus proliferation through multiple stages. Then the inhibitory effects of Gel-FeS NPs on PRRSV and the potential antiviral mechanism were explored. The results showed that Gel-FeS NPs could not only inactivate PRRSV directly in vitro, but also effectively inhibit the adsorption and invasion process of PRRSV, which blocked the virus outside cells, playing an important role in inhibition infection. According to the research findings, Gel-FeS NPs could inhibit infection by inhibiting the adsorption and invasion processes of PRRSV, which blocked viruses from entering host cells, in addition, it could also directly inactivate PRRSV in vitro, demonstrating the inhibitory effect at the initial stage of infection. As a kind of good biocompatible material, gelatin has been used in the research of drug delivery, wound adjuvant, vaccine adjuvant and so on [43–46]. The gelatin-modified nanoparticles prepared in this paper

can be further coated with antiviral drugs or modified functional molecules on their surface in the future to improve their targeting and antiviral effects.

Reactive oxygen species (ROS) as potential antiviral targets are by-products of cellular metabolism [47]. It is known that several viral infections cause an increase in intracellular ROS, which is mainly facilitated by viral-induced imbalances in the antioxidant defense mechanisms of the cell, which might activate certain host cellular pathways and promote viral replication [48, 49]. It has been shown that nano-sized iron (II) complex exhibited excellent radical-scavenging activities, and showed well antiviral activity against tobacco mosaic viruses (TMV) [50]. Hence, it was speculated that Gel-FeS NPs could also inhibit viral infection by mediating the level of ROS arisen from PRRSV infection. And the fluorescent probe DCFH-DA was used to detect the relative level of ROS induced by PRRSV infection. After treatment with Gel-FeS NPs, there is no significant difference in the intensity of the green fluorescence signal in the cells treated with Gel-FeS NPs (Supplementary Fig S2). The result showed that Gel-FeS NPs could not inhibit the ROS induced by PRRSV. Hydrogen peroxide can react with a range of targets and is only toxic when accumulated to high levels in the presence of redox metals (Fenton reaction) or O^{2-} (Haber–Weiss reaction), leading to the production of hydroxyl radicals [48]. The ferrous ions released by Gel-FeS NPs react with the reactive oxygen species induced by PRRSV, resulting in ferrous ions with antiviral activity and cannot reduce the cell's reactive oxygen levels.

Conclusion

In this work, we reported for the first time the virucidic and antiviral activity of Gel-FeS NPs. The Gel-FeS NPs with good dispersibility and biocompatibility were synthesized, and they exhibited effective inhibition on the proliferation of PRRSV by blocking the PRRSV outside the host cells. Moreover, the Fe^{2+} from degraded ferrous sulfide still displayed an antiviral effect, demonstrating the advantage as an antiviral nanomaterial of Gel-FeS NPs compared to other nanomaterials. This work highlighted the antiviral effect of Gel-FeS NPs, broaden the applications of iron-based nanoparticles for combating the virus.

Declarations

Acknowledgment

This research was supported by the National Natural Science Foundation of China (31772785, 31490602, 22074048).

Disclosure

The author reports no conflicts of interest in this work.

References

1. Lunney JK, Fang Y, Ladinig A, Chen N, Li Y, Rowland B, et al. Porcine reproductive and respiratory syndrome virus (PRRSV): Pathogenesis and interaction with the immune system. Annu Rev Anim Biosci. 2016;4:129–54.
2. Ma J, Ma LL, Yang MT, Wu W, Feng W, Chen Z. The function of the PRRSV-host interactions and their effects on viral replication and propagation in antiviral strategies. Vaccines. 2021;9(4):364.
3. Reina G, Peng S, Jacquemin L, Andrade AF, Bianco A. Hard nanomaterials in time of viral pandemics. ACS Nano. 2020;14(8):9364–88.
4. Lee J, Sands I, Zhang WX, Zhou LB, Chen YP. DNA-inspired nanomaterials for enhanced endosomal escape. Proc Natl Acad Sci U S A. 2021;118(19):e2104511118.
5. Mirtaleb MS, Mirtaleb AH, Nosrati H, Heshmatnia J, Falak R, Zolfaghari Emameh R. Potential therapeutic agents to COVID-19: An update review on antiviral therapy, immunotherapy, and cell therapy. Biomed Pharmacother. 2021;138:111518.
6. Yoon BK, Jeon WY, Sut TN, Cho NJ. Jackman JA. Stopping membrane-enveloped viruses with nanotechnology strategies: Toward antiviral drug development and pandemic preparedness. ACS Nano. 2021;15(1):125–48.
7. Chen L, Liang JG. An overview of functional nanoparticles as novel emerging antiviral therapeutic agents. Mater Sci Eng C Mater Biol Appl. 2020;112:110924.
8. Kwon PS, Ren S, Kwon SJ, Kizer ME, Kuo L, Xie M, et al. Designer DNA architecture offers precise and multivalent spatial pattern-recognition for viral sensing and inhibition. Nat Chem. 2020;12(1):26–35.
9. Park SJ, Kim J, Kang S, Cha HJ, Shin H, Park J, et al. Discovery of direct-acting antiviral agents with a graphene-based fluorescent nanosensor. Sci Adv. 2020;6(22):eaaz8201.
10. Anand A, Unnikrishnan B, Wei SC, Chou CP, Zhang LZ, Huang CC. Graphene oxide and carbon dots as broad-spectrum antimicrobial agents - a minireview. Nanoscale Horiz. 2019;4(1):117–37.
11. Muñoz A, Sigwalt D, Illescas BM, Luczkowiak J, Rodriguez-Perez L, Nierengarten I, et al. Synthesis of giant globular multivalent glycofullerenes as potent inhibitors in a model of Ebola virus infection. Nat Chem. 2016;8(1):50–7.
12. Ramos-Soriano J, Reina JJ, Illescas BM, de la Cruz N, Rodriguez-Perez L, Lasala F, et al. Synthesis of highly efficient multivalent disaccharide/[60]fullerene nanoballs for emergent vruses. J Am Chem Soc. 2019;141(38):15403–12.
13. Rodríguez-Pérez L, Ramos-Soriano J, Pérez-Sánchez A, Illescas BM, Munoz A, Luczkowiak J, et al. Nanocarbon-based glycoconjugates as multivalent inhibitors of Ebola virus infection. J Am Chem Soc. 2018;140(31):9891–8.
14. Kwon SJ, Na DH, Kwak JH, Douaisi M, Zhang F, Park EJ, et al. Nanostructured glycan architecture is important in the inhibition of influenza A virus infection. Nat Nanotechnol. 2017;12(1):48–54.
15. Wang CG, Guan YK, Lv MZ, Zhang R, Guo Z, Wei X, et al. Manganese increases the sensitivity of the cGAS-STING pathway for double-stranded DNA and is required for the host defense against DNA viruses. Immunity. 2018;48(4):675–87.

16. Zheng J, Fan R, Wu H, Yao H, Yan Y, Liu J, et al. Directed self-assembly of herbal small molecules into sustained release hydrogels for treating neural inflammation. Nat Commun. 2019;10:1604.
17. Dey P, Bergmann T, Cuellar-Camacho JL, Ehrmann S, Chowdhury MS, Zhang M, et al. Multivalent flexible nanogels exhibit broad-spectrum antiviral activity by blocking virus entry. ACS Nano. 2018;12(7):6429–42.
18. Schmitz A, Weber A, Bayin M, Breuers S, Fieberg V, Famulok M, et al. A SARS-CoV-2 spike binding DNA aptamer that inhibits pseudovirus infection by an RBD-independent mechanism. Angew Chem Int Ed. 2021;60(18):10279–85.
19. Jones ST, Cagno V, Janecek M, Ortiz D, Gasilova N, Piret J, et al. Modified cyclodextrins as broad-spectrum antivirals. Sci Adv. 2020;6(5):eaax9318.
20. Fraga CG, Oteiza PI. Iron toxicity and antioxidant nutrients. Toxicology. 2002;180(1):23–32.
21. Abdel-Rahman LH, Abu-Dief AM, Newair EF, Hamdan SK. Some new nano-sized Cr(III), Fe(II), Co(II), and Ni(II) complexes incorporating 2-((E)-(pyridine-2-ylimino)methyl)napthalen-1-ol ligand: Structural characterization, electrochemical, antioxidant, antimicrobial, antiviral assessment and DNA interaction. J Photochem Photobiol B. 2016;160:18–31.
22. Sagripanti JL, Routson LB, Lytle CD. Virus inactivation by copper or iron ions alone and in the presence of peroxide. Appl Environ Microbiol. 1993;59(12):4374–6.
23. Terpilowska S, Siwicki AK. Chromium(III) and iron(III) inhibits replication of DNA and RNA viruses. Biometals. 2017;30(4):565–74.
24. Zhu YB, Tong LQ, Nie KX, Wiwatanaratanabutr I, Sun P, Li Q, et al. Host serum iron modulates dengue virus acquisition by mosquitoes. Nat Microbiol. 2019;4(12):2405–15.
25. Wang HB, Li Z, Niu JL, Xu Y, Ma L, Lu A, et al. Antiviral effects of ferric ammonium citrate. Cell Discov. 2018;4:14.
26. Urso K, Martínez-Bujanda JL, del Prado JM. Iron protein succinylate in the management of iron deficiency anemia: A comparative study with ferrous sulphate at low and high therapeutic doses. Nutrients. 2021;13(3):968.
27. Okonko DO, Grzeslo A, Witkowski T, Mandal AK, Slater RM, Roughton M, et al. Effect of intravenous iron sucrose on exercise tolerance in anemic and nonanemic patients with symptomatic chronic heart failure and iron deficiency FERRIC-HF: A randomized, controlled, observer-blinded trial. J Am Coll Cardiol. 2008;51(2):103–12.
28. Liu Y, Li Y, Kang H, Jin T, Jiao LF. Design, synthesis, and energy-related applications of metal sulfides. Mater Horiz. 2016;3(5):402–21.
29. Chen YN, Liang WY, Li YP, Wu Y, Chen Y, Xiao W, et al. Modification, application and reaction mechanisms of nano-sized iron sulfide particles for pollutant removal from soil and water: A review. Chem Eng J. 2019;362:144–59.
30. Dong ZX, Meng XY, Yang W, Zhang J, Sun P, Zhang H, et al. Progress of gelatin-based microspheres (GMSs) as delivery vehicles of drug and cell. Mater Sci Eng C-Mater Biol Appl. 2021;122:111949.

31. Xiong Z, He F, Zhao DY, Barnett MO. Immobilization of mercury in sediment using stabilized iron sulfide nanoparticles. Water Res. 2009;43(20):5171–9.
32. Li CM, Zheng LL, Yang XX, Wan XY, Wu WB, Zhen SJ, et al. DNA-AuNP networks on cell membranes as a protective barrier to inhibit viral attachment, entry and budding. Biomaterials. 2016;77:216–26.
33. Zhou YR, Tong T, Jiang XH, Fang LR, Wu Y, Liang JG, et al. GSH-ZnS nanoparticles exhibit high-efficiency and broad-spectrum antiviral activities via multistep inhibition mechanisms. ACS Appl Bio Mater. 2020;3(8):4809–19.
34. Du T, Zhang JY, Li CQ, Song T, Li P, Liu JF, et al. Gold/Silver Hybrid Nanoparticles with Enduring Inhibition of Coronavirus Multiplication through Multisite Mechanisms. Bioconjug Chem. 2020;31(11):2553–63.
35. Yang XX, Li CM, Huang CZ. Curcumin modified silver nanoparticles for highly efficient inhibition of respiratory syncytial virus infection. Nanoscale. 2016;8(5):3040–8.
36. Sun Y, Liu YL, Lou ZM, Yang K, Lv D, Zhou J, et al. Enhanced performance for Hg(II) removal using biomaterial (CMC/gelatin/starch) stabilized FeS nanoparticles: Stabilization effects and removal mechanism. Chem Eng J. 2018;344:616–24.
37. Shao DD, Ren XM, Wen J, Hu S, Xiong J, Jiang T, et al. Immobilization of uranium by biomaterial stabilized FeS nanoparticles: Effects of stabilizer and enrichment mechanism. J Hazard Mater. 2016;302:1–9.
38. Zhou LH, Wei XC, Ma ZJ, Mei B. Anti-friction performance of FeS nanoparticle synthesized by biological method. Appl Surf Sci. 2017;407:21–8.
39. Guo Y, Yao Z, Timmer BJJ, Sheng X, Fan L, Li Y, et al. Boosting nitrogen reduction reaction by bio-inspired FeMoS containing hybrid electrocatalyst over a wide pH range. Nano Energy. 2019;62:282–8.
40. Tong T, Hu HW, Zhou JW, Deng S, Zhang XT, Tang WT, et al. Glycyrrhizic-acid-based carbon dots with high antiviral activity by multisite inhibition mechanisms. Small. 2020;16(13):e1906206.
41. Duan EZ, Wang D, Fang LR, Ma J, Luo J, Chen H, et al. Suppression of porcine reproductive and respiratory syndrome virus proliferation by glycyrrhizin. Antiviral Res. 2015;120:122–5.
42. Du TF, Nan YC, Xiao SQ, Zhao Q, Zhou EM. Antiviral Strategies against PRRSV Infection. Trends Microbiol. 2017;25(12):968–79.
43. Chhabra R, Saha A, Chamani A, Schneider N, Shah R, Nanjundan M. Iron pathways and iron chelation approaches in viral, microbial, and fungal infections. Pharmaceuticals. 2020;13(10):275.
44. Drakesmith H, Prentice A. Viral infection and iron metabolism. Nat Rev Microbiol. 2008;6(7):541–52.
45. Zhang S, Cao YN, Yang Q. Transferrin receptor 1 levels at the cell surface influence the susceptibility of newborn piglets to PEDV infection. PLoS Pathog. 2020;16(7):e1008682.
46. Khan N, Chen X, Geiger JD. Role of divalent cations in HIV-1 replication and pathogenicity. Viruses. 2020;12(4):471.

47. Kim HO, Yeom MJ, Kim JY, Kukreja A, Na W, Choi JY, et al. Reactive Oxygen Species-Regulating Polymersome as an Antiviral Agent against Influenza Virus. Small. 2017;13(32):1700818.
48. Kanga JI, Park KM. Advances in gelatin-based hydrogels for wound management. J Mater Chem B. 2021;9(6):1503–20.
49. Hussain A, Hasan A, Babadaei MMN, Bloukh SH, Edis Z, Rasti B, et al. Application of gelatin nanoconjugates as potential internal stimuli-responsive platforms for cancer drug delivery. J Mol Liq. 2020;318:114053.
50. Rigueto CVT, Nazari MT, Massuda L, Ostwald BEP, Piccin JS, Dettmer A. Production and environmental applications of gelatin-based composite adsorbents for contaminants removal: a review. Environ Chem Lett. 2021;19:2465–86.

Figures

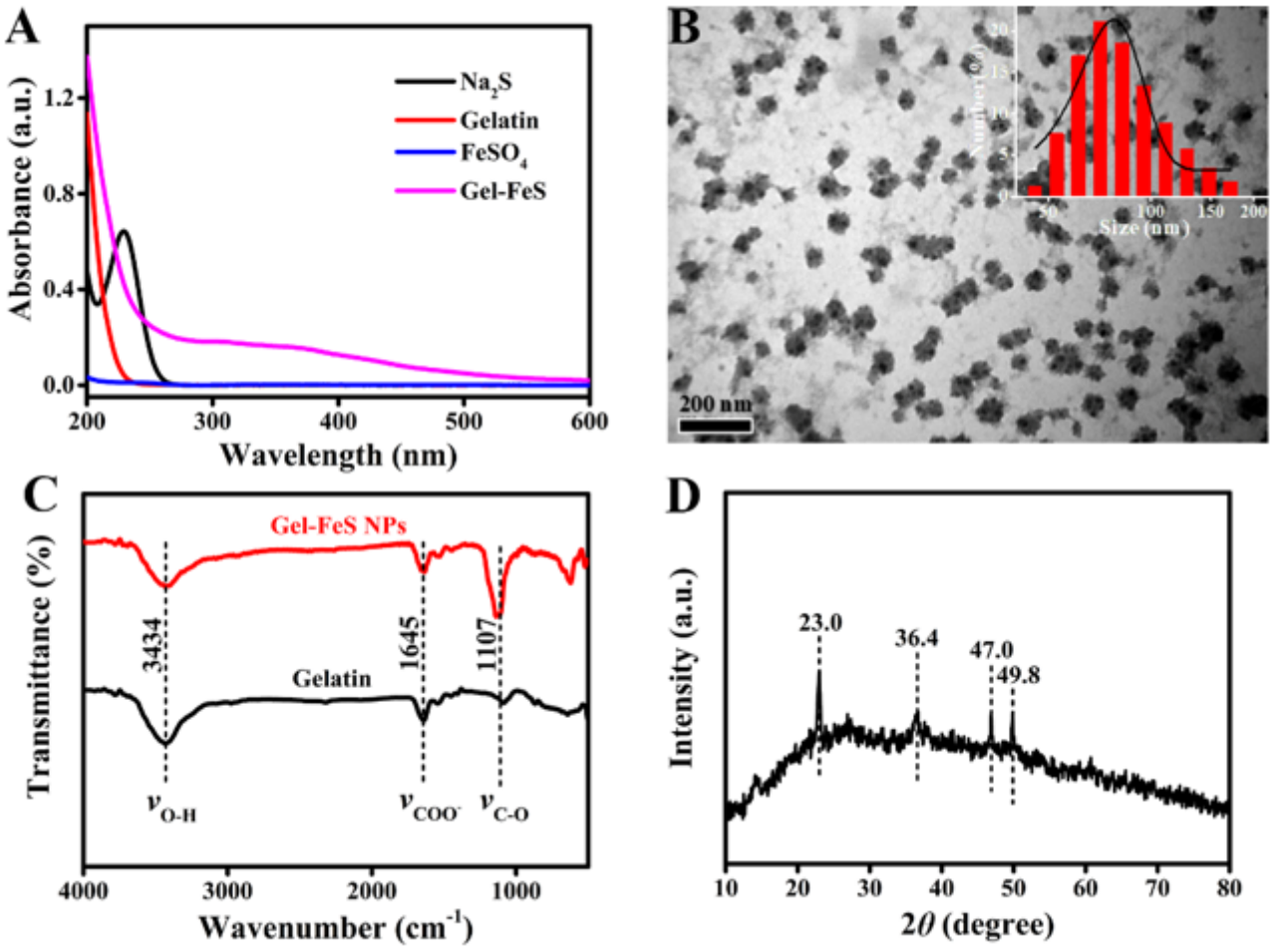

Figure 1

Characterization of the morphology and optical properties of Gel-FeS NPs (A) UV-Vis spectra of Gel-FeS NPs, FeSO4, Na2S and gelatin. (B) TEM image of the Gel-FeS NPs, inset in (B): DLS analysis of Gel-FeS

NPs. (C) FT-IR spectra of the Gel-FeS NPs and gelatin. (D) XRD pattern of Gel-FeS NPs.

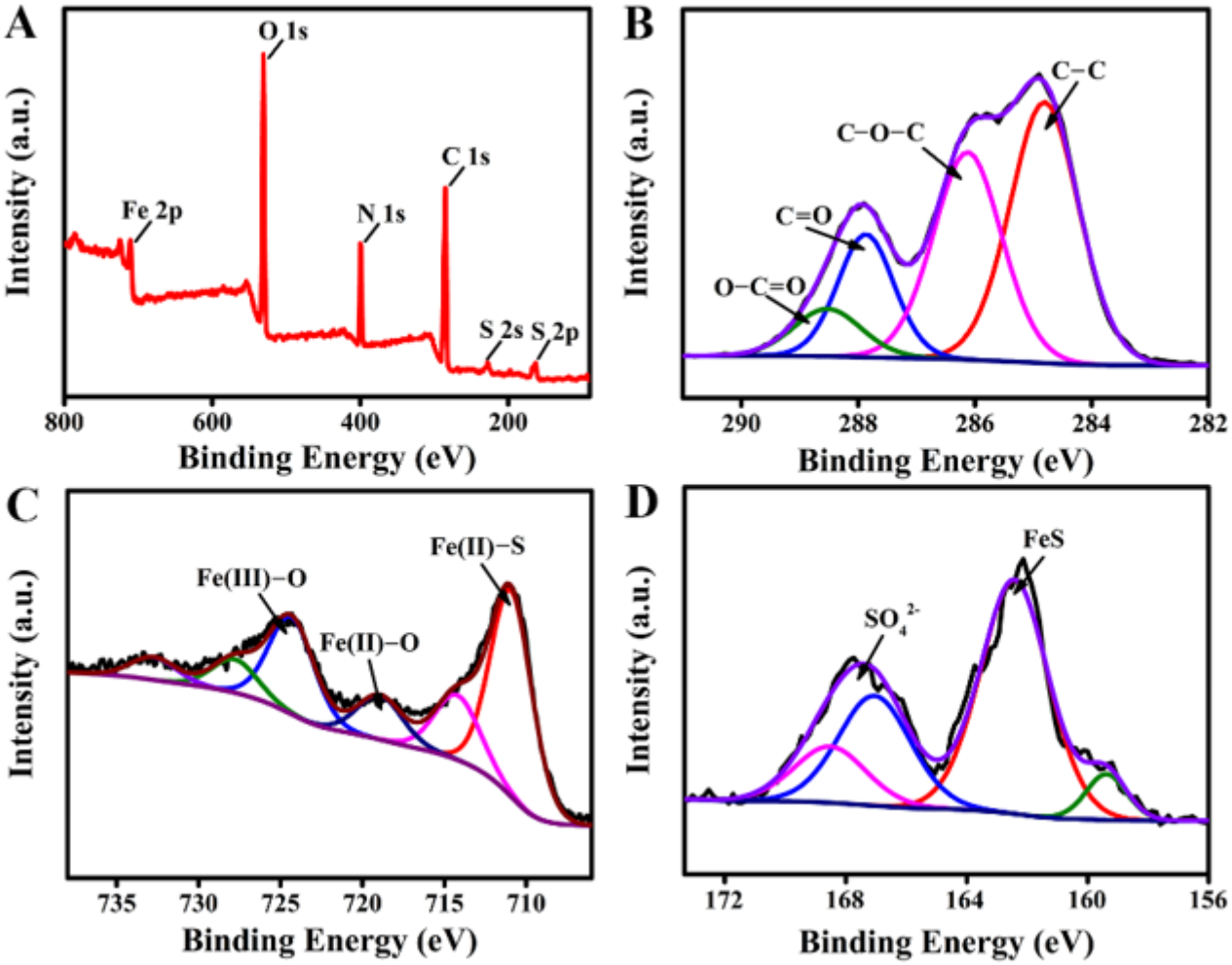

Figure 2

Photoelectron spectroscopy characterization of Gel-FeS NPs (A) XPS full scans spectrum of Gel-FeS NPs and high-resolution XPS spectra of (B) C 1s, (C) Fe 2p, (D) S 2p.

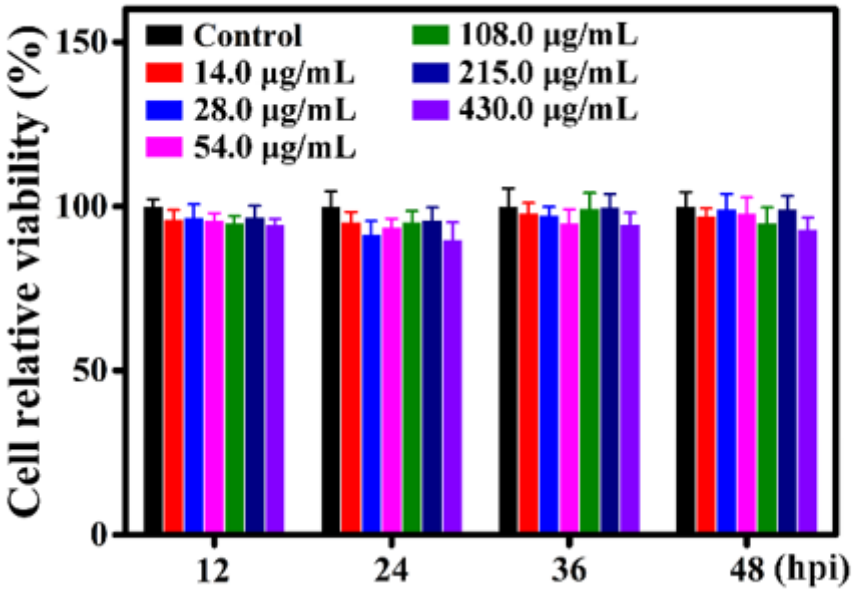

Figure 3

Cytotoxicity of different concentrations of Gel-FeS NPs (0–430 μg/mL) on MARC-145 cells by MTT assay. Error bars represent the standard deviation from three repeated experiments.

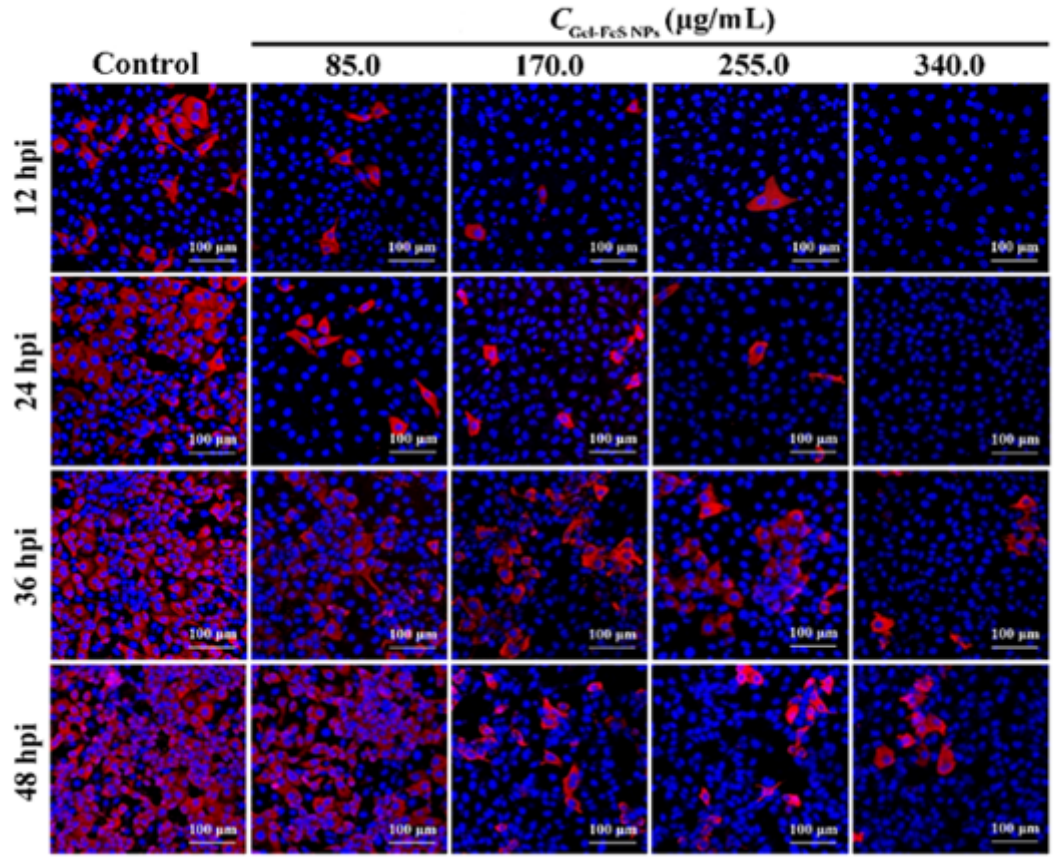

Figure 4

Quantitative analysis of the antiviral effect of Gel-FeS NPs through IFA. Immunofluorescence images of PRRSV-infected MARC-145 cells treated with different concentrations of Gel-FeS NPs (0–340.0 μg/mL). Scale bar = 100 μm.

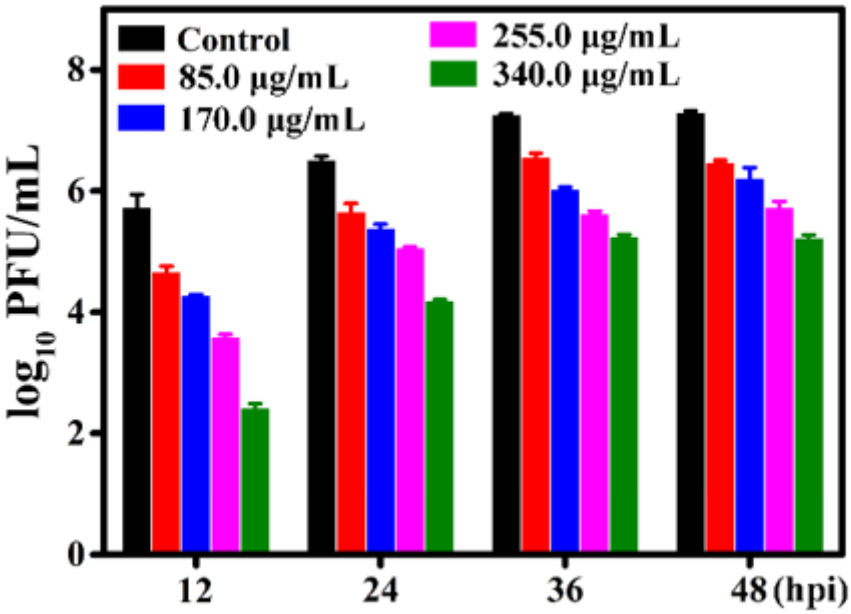

Figure 5

Titers of supernatant PRRSV treated with different concentrations of Gel-FeS NPs (0–340 μg/mL) detected by plaque assay. Error bars represent the standard deviation from three repeated experiments.

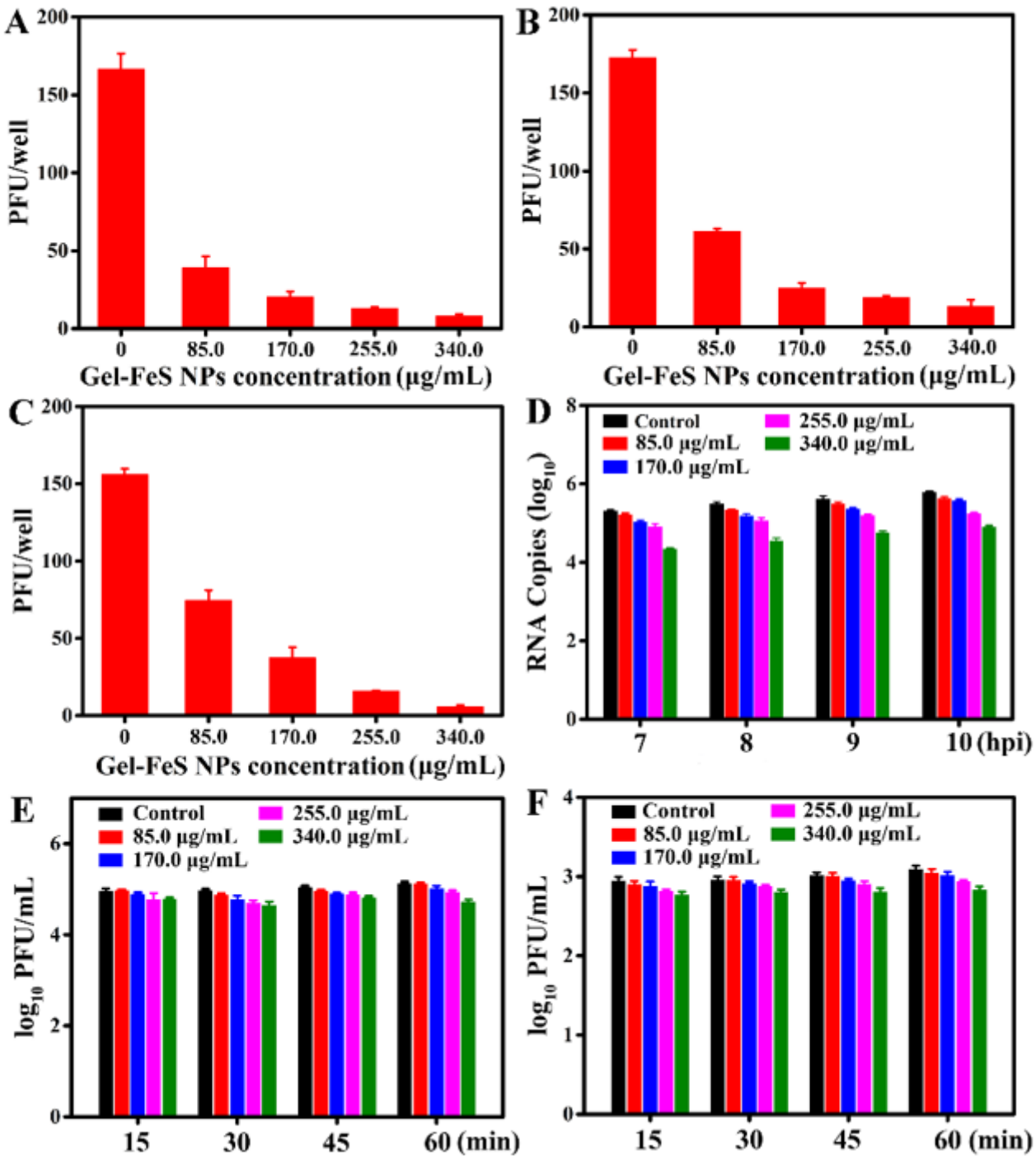

Figure 6

Multiple-stage effect of Gel-FeS NPs on PRRSV proliferation. (A) Inactivation effect of Gel-FeS NPs on PRRSV. The effect of Gel-FeS NPs on the infectivity of MARC-145 cells on the (B) adsorption, (C) invasion, (D) replication, (E) (F) release (intracellular and supernatant, respectively) processes of PRRSV infection.

Supplementary Files

This is a list of supplementary files associated with this preprint. Click to download.

- GraphicalAbstract.docx
- Supplementarymaterials.docx